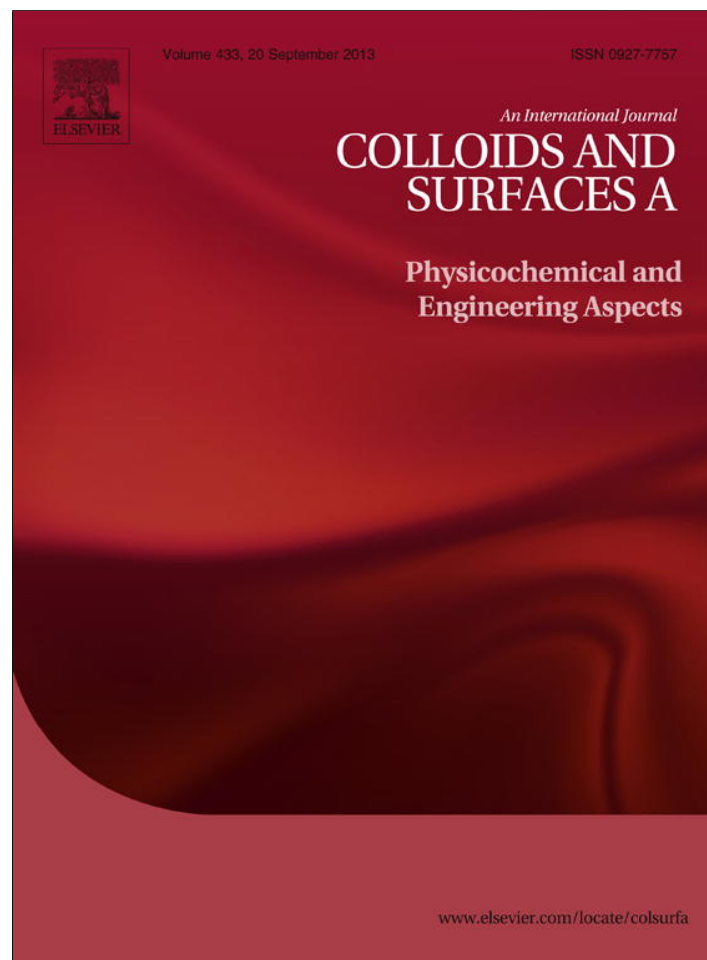


Provided for non-commercial research and education use.  
Not for reproduction, distribution or commercial use.



This article appeared in a journal published by Elsevier. The attached copy is furnished to the author for internal non-commercial research and education use, including for instruction at the authors institution and sharing with colleagues.

Other uses, including reproduction and distribution, or selling or licensing copies, or posting to personal, institutional or third party websites are prohibited.

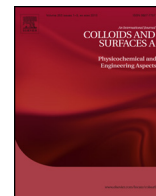
In most cases authors are permitted to post their version of the article (e.g. in Word or Tex form) to their personal website or institutional repository. Authors requiring further information regarding Elsevier's archiving and manuscript policies are encouraged to visit:

<http://www.elsevier.com/authorsrights>



Contents lists available at SciVerse ScienceDirect

# Colloids and Surfaces A: Physicochemical and Engineering Aspects

journal homepage: [www.elsevier.com/locate/colsurfa](http://www.elsevier.com/locate/colsurfa)

## Stability and interactions in mixed monolayers of fatty acid derivatives on Artificial Sea Water

A.M. Brzozowska<sup>1</sup>, F. Mugele, M.H.G. Duits\*

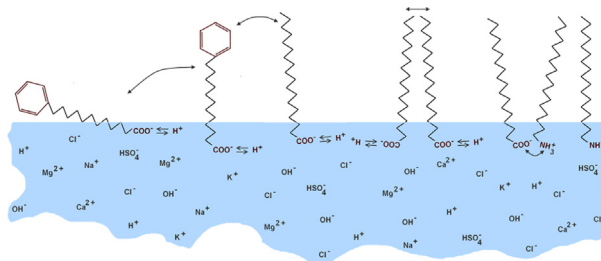
Physics of Complex Fluids group and MESA+ Institute, Faculty of Science and Technology, University of Twente, PO Box 217, 7500 AE, Enschede, The Netherlands

### HIGHLIGHTS

- Mixtures of stearic acid and stearyl amine at air/water interfaces show area contraction.
- Higher salinity of the sub-phase leads to stronger contraction and more stable mixed layers.
- Most stable mixtures are obtained for equal amounts of SA and SAM.
- Interfacial 12-phenyl dodecanoic acid (PDA) dissolves into the sub-phase at pH 7.
- Mixtures of SA and PDA show ideal mixing (weak interactions) at pH 3.

### GRAPHICAL ABSTRACT

Schematic representation of possible interactions between SA, SAM and PDA molecules at the air–liquid interface. The possible interactions include the followings: hydrophobic interactions between hydrocarbon and phenylated hydrocarbon chains, interactions between charged head groups, and interactions between charged head groups and counter-ions present in the sub-phase.



### ARTICLE INFO

#### Article history:

Received 21 February 2013

Received in revised form 23 April 2013

Accepted 23 April 2013

Available online 14 May 2013

#### Keywords:

Stearic acid

Stearyl amine

12-Phenyldodecanoic acid

Artificial Sea Water

Langmuir trough

Excess mixing area

Monolayer stability

### ABSTRACT

We studied the formation and stability of fatty acid and derivatives films on aqueous sub-phases by means of Langmuir trough experiments. Films were prepared from pure stearic acid (SA), stearyl amine (SAM) and 12-phenyldodecanoic acid (PDA), and from binary systems of SA with either SAM or PDA. For the aqueous sub-phase, multicomponent salt solutions ('Artificial Sea Water') at various concentrations ( $c_{ASW}$ , 0–100%) and pH values (3–7) were explored. SAM and SA differ most strongly at pH 7, where they can dissociate into oppositely charged species. For SA:SAM mixtures at this pH, pressure-area isotherms indicate mixing on a molecular scale. Increase of salt concentration from 0.05 to 0.5 M causes significant contraction of the layer, which is ascribed to (enhanced) electrostatic attractions between the head-groups. Relaxation experiments with these films indicate that dissolution of SAM into the sub-phase is suppressed by SA. The most stable films are formed at  $x_{SA} = 0.5$ , in agreement with the calculated excess free energy of mixing. PDA is much less amphiphilic than SA. (Meta-) stable mixed films of SA and PDA are formed only at high salt concentration and low pH, where the solubility of PDA into the sub-phase is the lowest. Under these conditions, SA appears to have a stabilizing effect, which is however not strong enough to prevent expulsion of PDA from interface. Isobars of SA:PDA films corroborate this picture. The weak interactions between SA and PDA are confirmed by the excess free energies of mixing, which are close to those of ideal mixtures.

© 2013 Elsevier B.V. All rights reserved.

\* Corresponding author at: University of Twente, Physics of Complex Fluids group and MESA+Institute, PO Box 217, 7500 AE, Enschede, The Netherlands.

Tel.: +31 53 4893097; fax: +31 53 4891096.

E-mail address: [m.h.g.duits@utwente.nl](mailto:m.h.g.duits@utwente.nl) (M.H.G. Duits).<sup>1</sup> Present address: Institute of Materials Research and Engineering, 3 Research Link, 117602 Singapore.

## 1. Introduction

Interfacial layers of amphiphilic hydrocarbons play a crucial role in enhanced oil recovery (EOR) [1–4]. These hydrocarbons naturally occur in adsorbed or chemically bonded states on rock surface [5–7], and in a dissolved state in crude oil [8–11]. When either the rock or the oil is brought into contact with an aqueous phase, new interfaces are created, providing opportunities for the amphiphiles to accumulate there. As a result, the deposited layers can desorb from the rock and disintegrate, therewith changing the wettability of the rock. In parallel, the adsorption of the amphiphiles at the oil/water interface can also lower the interfacial tension, with consequences for the manner in which the oil and aqueous phases co-exist at rest and in flow [11–15]. Although these adsorption-related key phenomena in EOR are well-known [16–20], questions still remain at the mechanistic level.

One important category hereof concerns the role of the water composition: how does the coexistence of different ions (especially the mono- and divalent cations) affect the integrity of adsorbed layers? It is known from studies in the field and in the lab that pH [21–29], overall salinity [3,21,30–32] (and sometimes even the presence of specific ions [22,23,28,33–41]) can strongly influence the ad- or desorption of amphiphilic species from interfaces with solid (S), oil (O) and air (A). Charge interactions play an important role, but it is not always clear how. The dissociation of the amphiphilic molecules is often governed by acid-base equilibria, but these equilibria can be shifted due to the electrical potential of the interface [25,42–48]. Polar solid substrates (like silica or mica) generally contribute to this potential via the dissociation of surface groups (e.g. [49–54]). For air or oil 'substrates' the potential is entirely set by the adsorption of the (charged) amphiphiles themselves.

In this paper we focus on air/water interfaces. This arguably more 'simple' system (compared to solid–water interfaces) allows focusing on the interactions of the amphiphilic molecules: (i) amongst themselves at the interface and (ii) with the ionic species in the sub-phase. The pH and salinity of the water will simultaneously influence both types of interactions. Previous studies with single component acidic amphiphiles (fatty acids) have addressed the effect of the hydrocarbon tail length, head group dissociation and counter-ion condensation on the 2D phase behaviour [25,42,44,55–75]. In a recent study, using (dilutions of) Artificial Sea Water, we found that the hydrophobic interactions between the tails dominate at low pH and low (but finite) salinity, leading to the formation of 3D solid phase. However, when the pH and/or the salinity is raised, charge interactions between the head-groups lead to suppression of this phase separation, and to an increased resistance against compression [29,76].

A second important category of questions concerns the coexistence of different types of amphiphilic molecules in crude oil (and hence also at interfaces). How do these different species interact, and how does this translate to the overall phase behaviour and mechanical properties of the interfacial layer? This type of question has hardly been addressed in the literature so far, although it is well known that crude oil contains a variety of amphiphilic components [8,77], and that the interfacial behaviour of amphiphilic mixtures can vary significantly, including synergistic or non-synergistic effects (e.g. [78–81]) affecting mechanical properties (stability) of the interfacial films (e.g. [82]). We address this issue in our present work, focusing at air/water interfaces and varying the aqueous composition. Here, we restrict ourselves to binary mixtures of amphiphiles. Inspired by the distinctions that can be made between the types of amphiphiles occurring in crude oil, we consider two mixtures.

In the first mixture, the difference between the two molecules lies entirely in the type of head-group, being carboxylic acid for

one, and amine for the other. The hydrophobic tail is an octadecyl chain. Individually, both stearic acid (SA) [29,62–64,83–85] and stearyl amine (SAm) [76,86–90] are relatively well characterised regarding their interfacial behaviour, but on their mixtures only few studies have been undertaken [78,91]. At (near-) neutral pH both molecules show partial dissociation, leading to oppositely charged head-groups. While this could lead to the formation of a molecularly mixed phase [78], also segregated phases of SA and SAm have been found [91], indicating meta-stable behaviour. An interesting question is how the strength of the attraction between the head-groups of interfacial SA and SAm compares to the interactions of these groups with the counter-ions in the aqueous sub-layer. Varying the salt concentration should provide a suitable way to study the relative importance of these interactions.

In the second mixture the head-group is carboxylic acid for both amphiphiles, but the hydrophobic tail is different: one has an octadecyl chain (SA) while the other one contains an aromatic group. By choosing 12-phenyldodecanoic acid (PDA), the number of carbon atoms is kept the same. SA and PDA could be regarded as simplistic representations of the naphthenate and asphaltene fractions in crude oil (we remark that this would be in the context of interfacial behaviour only, and that other model representations of crude oil fractions by single molecules have been proposed [92–95]). Despite having the same functional group and the same number of C-atoms in the tail, the interfacial behaviours of SA and PDA might be very different. The ability of PDA to form stable monolayers is expectedly governed by the properties of the hydrocarbon chain (rather than the functional group). Since the phenyl group of PDA is more 'bulky' than the octadecyl chain of SA, the interactions between the hydrophobic chains are expected to be less attractive for the PDA. Besides that, the amphiphilic character of PDA should be less strong since the phenyl group is more polar than the octadecyl group. While the behaviour of PDA at A/W interfaces has never been studied (as far as we know), some findings were published on phenylated fatty acids containing diacetyl groups. Yoshioka [96] reported that on water sub-phases at pH 6.8, the stability of monolayers of such molecules increases with number of CH<sub>2</sub>-groups separating the phenyl and diacetyl groups. As there is no diacetyl group in PDA, the molecules having the largest separation between the phenyl group and diacetyl group might offer the closest resemblance in behavior. The behavior of PDA:SA mixtures is more difficult to predict: the dissimilarities between PDA and SA might result in interfacial phase separation, but molecular mixing is also conceivable.

To study these interfacial phenomena, we performed experiments on a Langmuir trough. Isotherms were analysed for extracting information about the interactions between adsorbed species, both via the signature of the entire  $\pi$ -A curve, and via the specific molecular areas and pressures at which transitions are found. Moreover, they were also analysed for the excess free energy of mixing, as a function of the mixing ratio (and the salinity of the aqueous sub-layer). Isobars were measured to quantify the loss rate of material at selected values of the surface pressure. The dependence of these rates on the amphiphile mixing ratio and the sub-layer salinity were analysed to infer about which component is expelled from the layer, and what the mechanism might be. This work can be considered as a follow-up on a study in which we studied the interfacial behaviour of pure SA on a variety of Artificial Sea Water sub-phases [29].

In this paper, we will present clear indications that in SA:SAm mixtures, charge-induced contraction can take place, provided that the pH is near neutral, and that the amphiphiles are mixed at the molecular level. We will also show that in SA-PDA mixtures the interactions between the two amphiphiles are rather weak.

## 2. Materials and methods

### 2.1. Chemicals and solutions

Octadecanoic acid (stearic acid, grade 1, approx. 99%) was purchased from Sigma, octadecylamine (stearyl amine,  $\geq 99.0\%$ ) from Aldrich, and 12-phenyldodecanoic acid (PDA) from Rare Chemicals GmbH. 0.1 M standard solutions of NaOH and HCl were purchased from Fluka. Solutions of SA, SAm and PDA were prepared in  $\text{CHCl}_3$  (ACS reagent grade, Sigma–Aldrich) at concentrations of 1 mg/ml. Artificial Sea Water (ASW) is a 10 component mixture with total concentration of 0.53 M [22,97]. It consists of: NaCl (426 mM),  $\text{NaSO}_4$  (29.4 mM), KCl (9.45 mM),  $\text{NaHCO}_3$  (2.43 mM), KBr, (0.86 mM),  $\text{H}_3\text{BO}_3$  (0.44 mM), NaF (0.074 mM),  $\text{MgCl}_2$  (55.5 mM),  $\text{CaCl}_2$  (10.8 mM) and  $\text{SrCl}_2$  (0.094 mM). All these salts were of ACS reagent grade, purchased from Sigma, and used as received. Dilutions of ASW were prepared with ultrapure water (18.2 M $\Omega$ cm, Millipore Synergy UV system). The pH was adjusted with 0.1 M NaOH or 0.1 M HCl. Note that the change in concentration of  $\text{Na}^+$ ,  $\text{H}^+$ ,  $\text{Cl}^-$  and  $\text{OH}^-$  due to pH adjustment was very small even for 100 times diluted ASW. Experiments with (diluted) ASW sub-phases were concluded within 2 h after pH adjustment.

### 2.2. Experimental techniques

Two types of measurement were performed: pressure-area ( $\pi$ - $A$ ) isotherms and ( $A$ - $t$ ) isobars. These experiments, which are briefly explained (along with some definitions) in Fig. 1, were carried out using an automated Langmuir trough (NIMA model 1212D1) equipped with a pressure sensor and a dipper. Room temperature ( $22.5 \pm 0.5^\circ\text{C}$ ) and humidity were monitored continuously. To reduce contamination with dust and to ensure stable measurement conditions, the trough was placed on a floating table and surrounded by a home-built laminar flow box. The air flow in the box was stopped during measurements. Prior to experiments the trough was rigorously cleaned with pure water and chloroform. After filling the trough up with freshly prepared sub-phase, impurities were removed via suction of the top layer (using a NeoLab vacuum system). The interface was considered clean if the pressure change during consecutive compression and decompression of the interface was  $< 0.1$  mN/m.

In the preparation of the mixed films, we used a protocol based on the findings of Lee et al. [78]. These authors explored different ways of spreading SA:SAm mixtures and concluded that consecutive spreading of the individual components resulted in films with separate SA and SAm domains. This was evidenced by isotherms

with features characteristic for both individual components, and two collapse points (another hallmark of segregation could be the appearance of horizontal phase lines [76]). In the same study Lee et al. succeeded in making homogeneously mixed films, by premixing the molecules in solution prior to the spreading. We followed this protocol for both SA:SAm and SA:PDA mixtures.

Solutions of SA, SAm, PDA and the mixtures (all at total concentration of approximately 1 mg/ml in  $\text{CHCl}_3$ ) were spread using a 50  $\mu\text{L}$  Hamilton microsyringe on an enclosed sub-phase with an initial area  $S$  of 500–700  $\text{cm}^2$ , depending on the molecules (at the same spreading concentration, SAm and PDA occupy a larger area at low surface pressures than SA). After spreading the film was allowed to equilibrate for 30 min. Subsequently it was compressed at a constant rate  $dS/dt$  of  $-10 \text{ cm}^2/\text{min}$ . Meanwhile,  $\pi$  was measured continuously using a Wilhelmy plate (filter paper) attached to the pressure sensor. Given the trough area  $S$ , the area  $A$  per molecule was calculated assuming that no molecules had left the interface during compression. For each sub-phase composition, at least five  $\pi$ - $A$  isotherms were measured to ensure the reproducibility (typical examples are shown in the Supplementary Information). The isotherms were also used as a reference for defining the surface pressure in film relaxation measurements. In these isobaric experiments, which were typically performed twice per (pH,  $c_{\text{ASW}}$ ) condition, the monolayer was compressed to a target pressure  $\pi$  at  $dS/dt$  of  $-10 \text{ cm}^2/\text{min}$ , after which the constant pressure was maintained by automatic adjustment of the film area. Iso-bars of the most stable films were recorded up to several hours.

## 3. Results and discussion

One of the key compounds in this work, stearic acid, has been elaborately examined in a previous study [29], using the same techniques and addressing the same (pH,  $c_{\text{ASW}}$ ) conditions for the aqueous sub-phase. Those  $\pi$ - $A$  isotherms that are indispensable for interpretation of the behaviour of the mixed films, are also included in the present paper.

### 3.1. Stearyl amine – the effect of functional group

#### 3.1.1. Pressure-area isotherms of SAm (+SA)

SA:SAm monolayers were studied at sub-phase pH 7. At this condition, it is likely that both molecules are partially dissociated giving rise to opposite charges ( $\text{R-COO}^-$  and  $\text{R-NH}_3^+$ ). The precise degree of dissociation  $\alpha$  should depend on the intrinsic  $\text{pK}_a$  values of the molecules ( $\sim 5.4$  for long-chain fatty acids [98] and  $\sim 10.6$  for long-chain fatty amines [99]), the bulk pH, the bulk

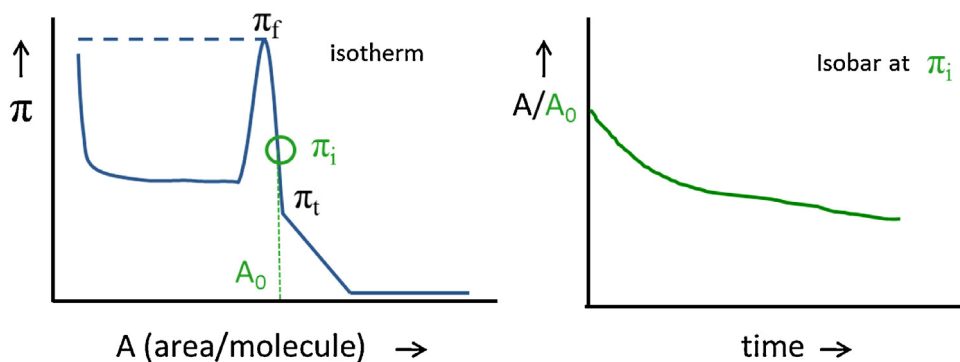


**Fig. 1.** Schematic drawing of experiments on fatty acid monolayers on a Langmuir trough. Left:  $\pi$ - $A$  isotherm. Upon compression, the film undergoes several phase transitions, where the type of phase can differ per fatty acid. Generally a transition to a steep part can be identified; the corresponding surface pressure is denoted as  $\pi_t$  in this paper. When  $A$  reaches the area corresponding to the closest packing, the layer undergoes fracture at pressure  $\pi_t$ . For even smaller areas, two collapse signatures are distinguished: a constant area collapse (solid line) and a constant pressure collapse (dashed line). Right:  $A(t)$  isobar. Compression is continued until a set point of  $\pi$  is reached, after which this  $\pi$  is maintained by adjusting the film area  $A$ . Generally  $A(t)$  decreases due to loss of molecules from the interface.  $A_0 = A(t=0)$  is the area at the time where the set point pressure was reached.

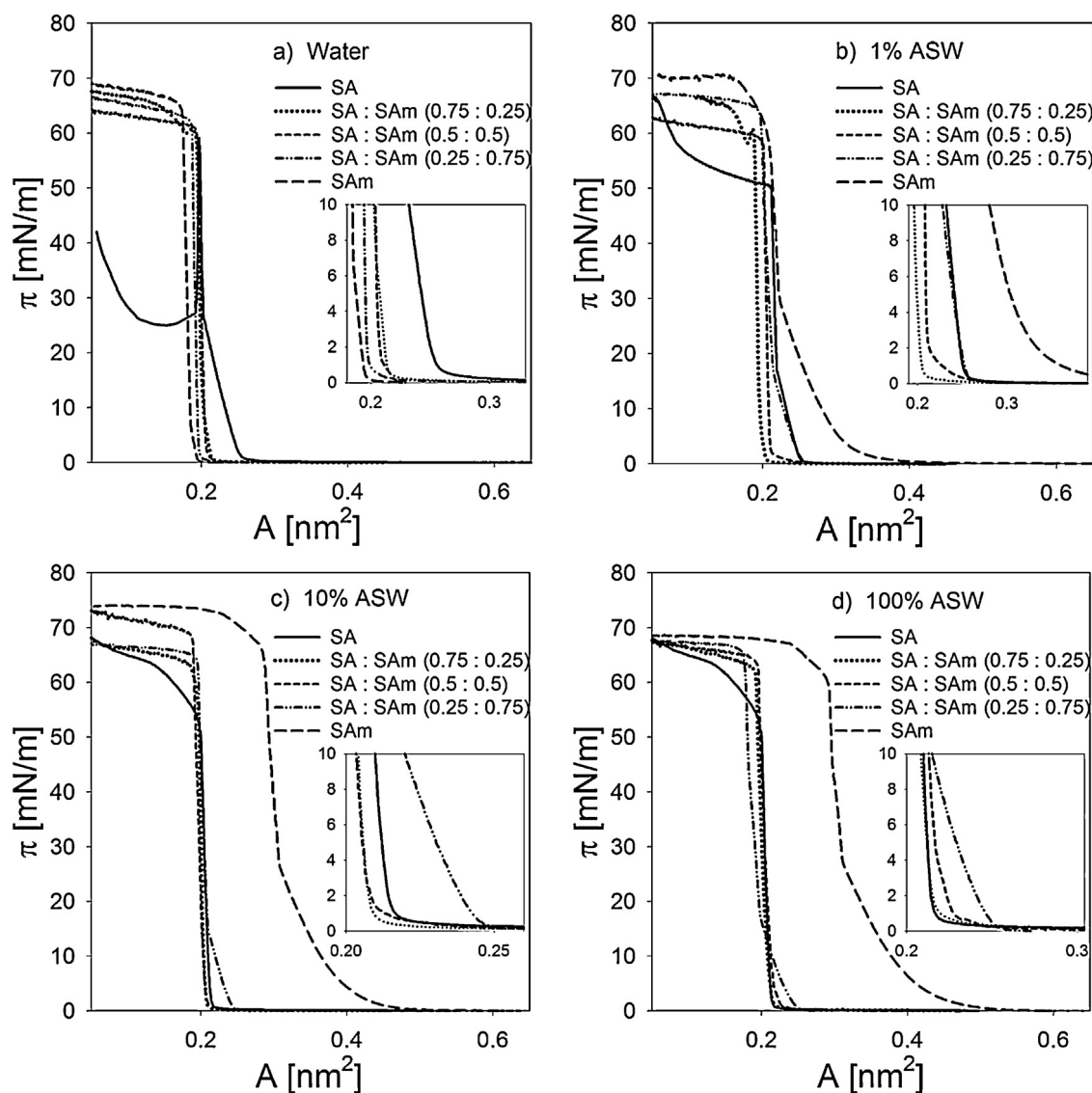


**Fig. 2.**  $\pi$ -Isotherms of mixed stearic acid (SA) and stearyl amine (SAm) films at pH 7 on Artificial Sea Water sub-phases of varying ASW concentration. The concentration of  $\text{Na}^+$  ions in the pure water sub-phase due to pH adjustment is 0.09 mM. Insets show initial phase transitions upon compression of the films.

salt concentration and the local surface potential  $\psi$  [45]. As a result of the latter, the local pH at the interface might differ from that in bulk. Pressure-area ( $A$ - $\pi$ ) isotherms were measured for SA:SAm mixtures at three different mixing ratios, on sub-phases at 4 different salt concentrations. As a reference also measurements for pure SA and SAm were done. The isotherms are shown in Fig. 2.

First, we discuss the pure SAm films. On the 'pure water' sub-phase, i.e. in the absence of ASW-salt (Fig. 2a, dashed curve), the initial increase in  $\pi$  during film compression is observed at an area  $A$  below  $0.2 \text{ nm}^2$ , indicating a partial solubility of SAm in water as reported elsewhere [87,100]. Upon further compression we observe a 'liquid-condensed' to 'solid' transition at  $\pi \sim 7 \text{ mN/m}$ , in agreement with results of Lee et al. [78] and Albrecht et al. [76]. Film fracture occurs at  $\pi \sim 64 \text{ mN/m}$ , which is lightly higher than the fracture pressure of a pure SA film ( $\pi \sim 60 \text{ mN/m}$ ) [29]. The shape of the isotherm beyond the point of film fracture indicates a 'constant pressure collapse' mechanism.

As  $c_{\text{ASW}}$  is increased (Fig. 2b–d, dashed curves) the SAm monolayer expands, as evidenced by the appearance of the initial pressure-increase at a much larger  $A$ . A similar trend was found for SA films, although there the effect was much smaller [29]. We attribute this difference to the effective sizes of the head-groups.

The head-group of a bare  $\text{SAm}^+$  cation occupies significantly less space than that of an  $\text{SA}^-$  anion, making the charge density of the fatty cation higher. As a result the counter-ions bind more strongly to the  $\text{SAm}^+$  than to the  $\text{SA}^-$ . In turn, this stronger binding of counter-ions results in a larger hydration shell. Hence the overall effect is that SAm, due to its large head-group including counter-ions and hydration shell, occupies a larger interfacial area than SA.

The increasing expansion of the SAm monolayer as  $c_{\text{ASW}}$  is raised from 0% to 100% (Fig. 2a–d) is ascribed to an enhanced degree of dissociation ( $\alpha$ ) of the amine groups. The latter is known to happen at high salt concentrations, in particular in the presence of strongly binding  $\text{Cl}^-$  and  $\text{Br}^-$  ions [86], both of which are present in ASW. Most likely, the increased (average) molecular area is then a direct effect of the more 'bulky' head-group that now contains a bigger hydration shell and a bound counter-ion. The alternative explanation of an increased electrostatic repulsion between dissociated  $\text{SAm}^+$  groups is less likely since the increased  $c_{\text{ASW}}$  should enhance the charge screening.

Also the location  $A(\pi_t)$  of the 'liquid–solid' phase transition shows a dependence on salt concentration. For 1% ASW this transition occurs at  $A \sim 0.23 \text{ nm}^2/\text{molecule}$  while for  $c_{\text{ASW}} > 10\%$  it is found at  $A \sim 0.33$  to  $0.34 \text{ nm}^2$ . The corresponding  $\pi_t$  values at 1%, 10% and

100% ASW are 31, 27 and 27 mN/m, respectively. These increased  $\pi_t$  and  $A(\pi_t)$  values (as compared to SAM on pure water) correlate well with the appearance of an “liquid expanded” phase at high  $c_{ASW}$ .

An additional phase transition induced by ASW salt is observed at  $\sim 58, 66$  and  $60$  mN/m for 1%, 10% and 100% ASW, respectively. This transition, which is sharp for 10% and 100% ASW, may correspond to a rearrangement of the molecular packing within the solid phase. At even higher  $\pi$  film fracture occurs following a ‘constant pressure collapse’ model.

We now consider the isotherms of the mixed films. The isotherms on ‘pure’ water, at three different mixing ratios ( $x_{SA} = 0.25$ – $0.75$  with  $x_{SA}$  being the molar fraction of SA), show similar features to the isotherms of pure SAM and SA. At  $c_{ASW} = 0$  (Fig. 2a) we observe that the initial pressure increase upon film compression occurs at areas  $A$  between those of pure SA and SAM films, in agreement with work of Lee et al. [78]. This trend however, is not found on sub-phases of ASW (Fig. 2b–d). At 1% ASW the isotherms of the mixed films are shifted towards smaller  $A$  than SA and SAM isotherms. At 10% ASW only the isotherm with excess SAM lies between the SA and SAM isotherms. And at 100% ASW only parts of the isotherms below  $\pi \sim 10$  mN/m lie between the isotherms of the pure compounds.

We attribute the more dense molecular packing in the mixtures to the formation of complexes between the oppositely charged SA and SAM. In this scenario, the depletion of counter-ions and reduction of the hydration shell lead to the film contraction. The observation that at each  $c_{ASW} > 0$  the measured  $\pi_t$  (‘liquid to solid’ transition) decreases with increasing  $x_{SA}$ , corroborates that SA–SAM complexes are formed: in the case of segregated SA and SAM phases  $\pi_t$  would remain constant as in [91]. Also inspection (for a few samples) of the morphology of Langmuir Blodgett layers did not provide any indications for segregation (see Appendix). In Section 3.1.2 additional evidence based on the excess area of the mixed films will be presented.

We note that the isotherms of mixed films on 1%, 10% and 100% ASW show signatures of the component in excess. For example the isotherms at  $x_{SA} = 0.25$  show an ‘expanded liquid’ behaviour similar to pure SAM, albeit that it is less pronounced (see insets of Fig. 2c and d). Conversely, the mixture with  $x_{SA} = 0.75$  appears to behave similar to the pure SA film (clearly visible in Fig. 2c and d). Remarkably, the mixed films with  $x_{SA} = 0.5$  seem to behave more like films containing excess SA (Fig. 2c and d). We have no tentative explanation for that. Finally, we remark that the pressure at which film fracture occurs, increases with the concentration of SAM molecules in the film ( $x_{SA}$ ), independent of  $c_{ASW}$ .

### 3.1.2. Mixing and complexation between SA and SAM molecules

To examine the quality of mixing and the molecular interactions between SAM and SA, we analysed the excess areas ( $A_{ex}$ ) of the mixed SA:SAM films at surface pressures below  $\pi_t$ .  $A_{ex}$  is defined as:

$$A_{ex} = A_{SA/SAM} - A_{id} = A_{SA/SAM} - (X_{SA}A_{SA} + X_{SAM}A_{SAM}) \quad (1)$$

where  $A_{SA/SAM}$  is the area per molecule in the mixed film, whereas  $A_{SA}$  and  $A_{SAM}$  are similarly defined for the individual components.  $A_{id}$  corresponds to an ideally mixed film, i.e. without excess mixing area.

The results shown in Fig. 3 reveal several trends: (i)  $A_{ex}$  is negative under almost all ( $x_{SA}$ ,  $c_{ASW}$ ) conditions; (ii) at constant  $c_{ASW}$ ,  $A_{ex}$  becomes closer to zero with increasing surface pressure; (iii) at constant  $\pi$ ,  $A_{ex}$  becomes more negative as  $c_{ASW}$  increases (from comparisons in between the different graphs); and (iv) the  $x_{SA}$  value where  $A_{ex}$  is most negative, shifts from 0.75 at  $c_{ASW} = 0$  to 0.25 at  $c_{ASW} = 100\%$ . Regarding observation (i) we note that in the complete absence of salt, Lee et al. found predominantly positive  $A_{ex}$

values for their SA:SAM mixtures (Figure 7b in ref. [78]). This could indicate that the small amount of NaOH used to raise the pH to 7 already gave a negative contribution to  $A_{ex}$ .

To better understand the interactions between the molecules we calculated the excess free energy of mixing ( $\Delta G^E$ ) using the method of Goodrich [101], who showed that  $\Delta G^E$  can be calculated from the  $\pi$ – $A$  isotherms of the single components and mixed film by calculating areas under the curves:

$$\Delta G^E = N_A \left[ \int_{\pi^*}^{\pi} A_{SA/SAM} d\pi - X_{SA} \int_{\pi^*}^{\pi} A_{SA} d\pi - X_{SAM} \int_{\pi^*}^{\pi} A_{SAM} d\pi \right] \quad (2)$$

where  $N_A$  is Avogadro’s number. The lower integration limit  $\pi^*$  corresponds to pressure below which the molecules may be assumed to mix ideally [101,102]. The higher integration limit  $\pi$  corresponds to the pressure of interest. We performed calculations for  $\pi = 1$ – $50$  mN/m. Knowing the energy of ideal mixing  $\Delta G^{id}$  (Eq. (3)) we calculated the free energy of mixing (Eq. (4)) for each film composition:

$$\Delta G^{id} = RT(X_{SA} \ln(X_{SA}) + X_{SAM} \ln(X_{SAM})) \quad (3)$$

$$\Delta G^M = \Delta G^{id} + \Delta G^E \quad (4)$$

where  $R$  is the gas constant [J/(K mol)] and  $T$  is the temperature [K]. The results are shown in Fig. 4. We observe that the free energy of mixing reaches a minimum at  $x_{SA} = 0.5$  for all  $c_{ASW}$ , irrespective of the surface pressure. In the absence of ASW-salt, the minimum in  $\Delta G^M$  decreases from  $\sim -1.5$  to  $-2.0$  kJ/mol (corresponding to  $\sim -(0.6$ – $0.8) k_B T$  per molecule) as  $\pi$  is increased from 1 to 50 mN/m. In the presence of ASW-salt, similar trends are found, albeit that the minimum in  $\Delta G^M$  now decreases from  $-1.5$  to  $-2.5$  kJ/mole, regardless of the value of  $c_{ASW}$ .

These results can be interpreted as follows. First of all,  $\Delta G^M < 0$  indicates that the mixed SA:SAM films are more stable than the single-component films. The location of the  $\Delta G^M(x_{SA})$  minimum corresponds to the film composition where the interactions between SA and SAM are the strongest. Considering the formation of  $SA^-$  and  $SAM^+$  at pH 7, it is not unexpected to find the minimum  $\Delta G^M$  at  $x_{SA} = 0.5$ . The increasing depth of the minimum  $\Delta G^M$  as  $\pi$  is increased seems to be in line with stronger electrostatic attractions between the two species as the distance between the decreases.

The observation that  $\Delta G^M$  hardly depends on  $c_{ASW}$  indicates that the interactions between  $SA^-$  and  $SAM^+$  are stronger than those between the fatty ions and the counterions present in the ASW sub phase.

### 3.1.3. Film relaxation curves of SAM (+SA)

The film stability was further examined via film relaxation studies. Separate measurements were performed to study the stability of SAM and mixed SA:SAM monolayers. After compressing the films to  $\pi = 30$  or  $50$  mN/m, the pressure was held constant by adjusting the film area  $A$  when necessary.

The results are shown in Fig. 5. We find that for pure SAM and mixed SA:SAM films at  $x_{SA} = 0.25$ , the logarithm of  $A(t)/A_0$  scales initially with  $t^{1/2}$ , and in later stages with  $t$ . These behaviours are in good agreement with Ter Minnasian’s model [103] for diffusion of (in our case SAM) molecules into the sub-phase (more details can be found in the Supplementary Information). The loss rate is found to decrease as  $c_{ASW}$  is increased (except for pure SAM at 1% ASW, for which we have no tentative explanation). The clear dependence of the loss-rates on  $x_{SA}$  suggests that when there is insufficient SA to ‘bind’ all the SAM, the excess SAM tends to dissolve into the sub-phase. ASW cations then provide extra stabilisation through the formation of metal (M)–SAM complexes, which are more strongly adsorbed at the interface.

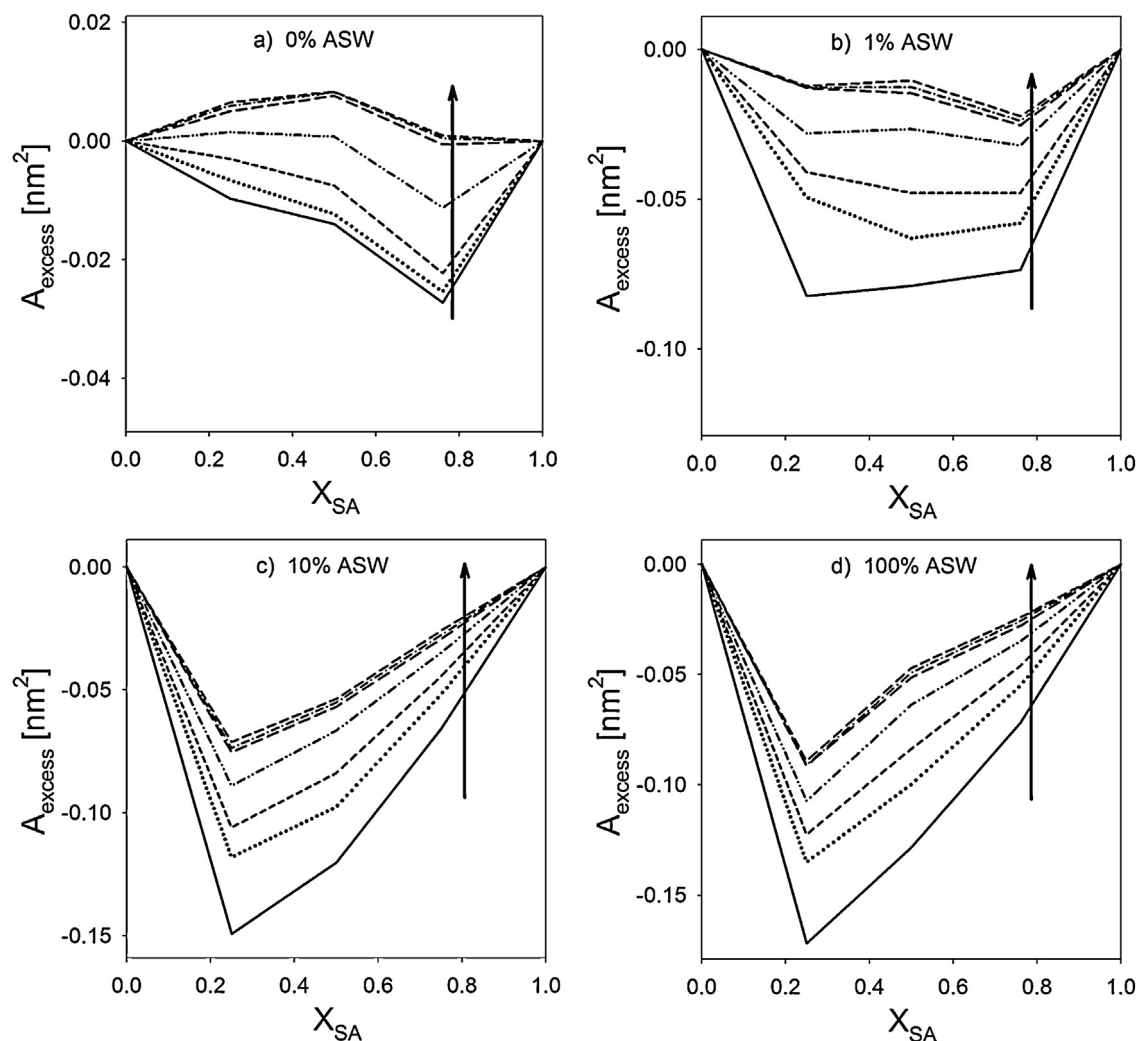


**Fig. 3.** Calculated excess area per molecule ( $A_{ex}$ ) as a function of composition of mixed SA:SAm films on sub-phases of varying  $c_{ASW}$  and pH 7.  $X_{SA}$  is a molar fraction of SA in the film. The arrows indicate the increase of the surface pressure. (—) 1 mN/m, (●●●●) 5 mN/m, (---) 10 mN/m, (-●-●-●) 20 mN/m, (- - -) 30 mN/m, (-●-●-) 40 mN/m, (- - -) 50 mN/m.

For  $x_{SA} = 0$  and 0.5 we abstained from a quantitative analysis of the loss rate, since the areas of the corresponding films remained practically constant in time; see Fig. 5e and f for  $x_{SA} = 0.50$ , and Fig. 5c and d in ref. [29] for pure SA films (except for  $c_{ASW} = 0$  where nucleation of SA into 3D solid was found). The strong dependence of the relaxation behaviour on the SA content further corroborates the occurrence of strong attractive interactions between the SA<sup>-</sup> and the SAm<sup>+</sup> species. This stabilises the film against the loss of molecules into the sub-phase.

### 3.2. 12-Phenyldodecanoic acid – effect of hydrophobic chain

#### 3.2.1. Pressure-area isotherms of PDA (+SA)

While  $\pi$ - $A$  isotherms could be measured, significant losses of PDA from the interface occurred during the measurements; sometimes even at low  $\pi$ . Hence the isotherms show qualitative trends but should not be regarded as ‘equilibrium data’.

First we consider the behaviour of pure PDA films. Fig. 6 shows  $\pi$ - $A$  isotherms on ‘pure’ water sub-phases at various pH values. At pH 7 where the carboxylic groups are (partly) dissociated, only a very small increase of the surface pressure can be detected during film compression. This indicates that substantial amounts of PDA get depleted into the sub-phase, either during the equilibration time, or during compression at low  $\pi$ . When the pH is lowered,

we observe an increasing tendency of the PDA molecules to stay at the interface. For pH  $\leq 5$ , measurable surface pressures are first encountered around  $A \sim 0.8 \text{ nm}^2$  and also a maximum in the  $\pi(A)$  curve is found. The magnitude of this  $\pi$ , which we interpret as a fracture pressure, is much smaller than the corresponding values found for SA films. When the pH is lowered from 5 to 3, this  $\pi_f$  decreases.

Clearly and as expected, pure PDA is unable to form strong interfacial layers on water sub-phases under discussed conditions: the maximum  $\pi$  that can be sustained is only  $\sim 10 \text{ mN/m}$ . Whether this value is reached depends on the pH of the sub-phase (and possibly also on the compression speed). In either case, the PDA turns out to be much less amphiphilic than SA. Apparently, the polarity of the phenyl-group strongly diminishes the ‘affinity contrast’ between the head and the tail of the molecule, thereby increasing the tendency to dissolve in the aqueous sub-phase. The pH-dependence of the PDA isotherms is believed to result from two effects: (i) the increased deprotonation of the COOH group as the pH is raised, enhances the solubility in the water sub-phase (somewhat similar to SA [29]) and (ii) the interactions between the (remaining) adsorbed PDA species become more repulsive due to this increased charging.

Next we consider the mixed SA:PDA films. In Fig. 7, we compare the  $\pi$ - $A$  isotherms of pure and mixed SA:PDA films at pH 3 (top)

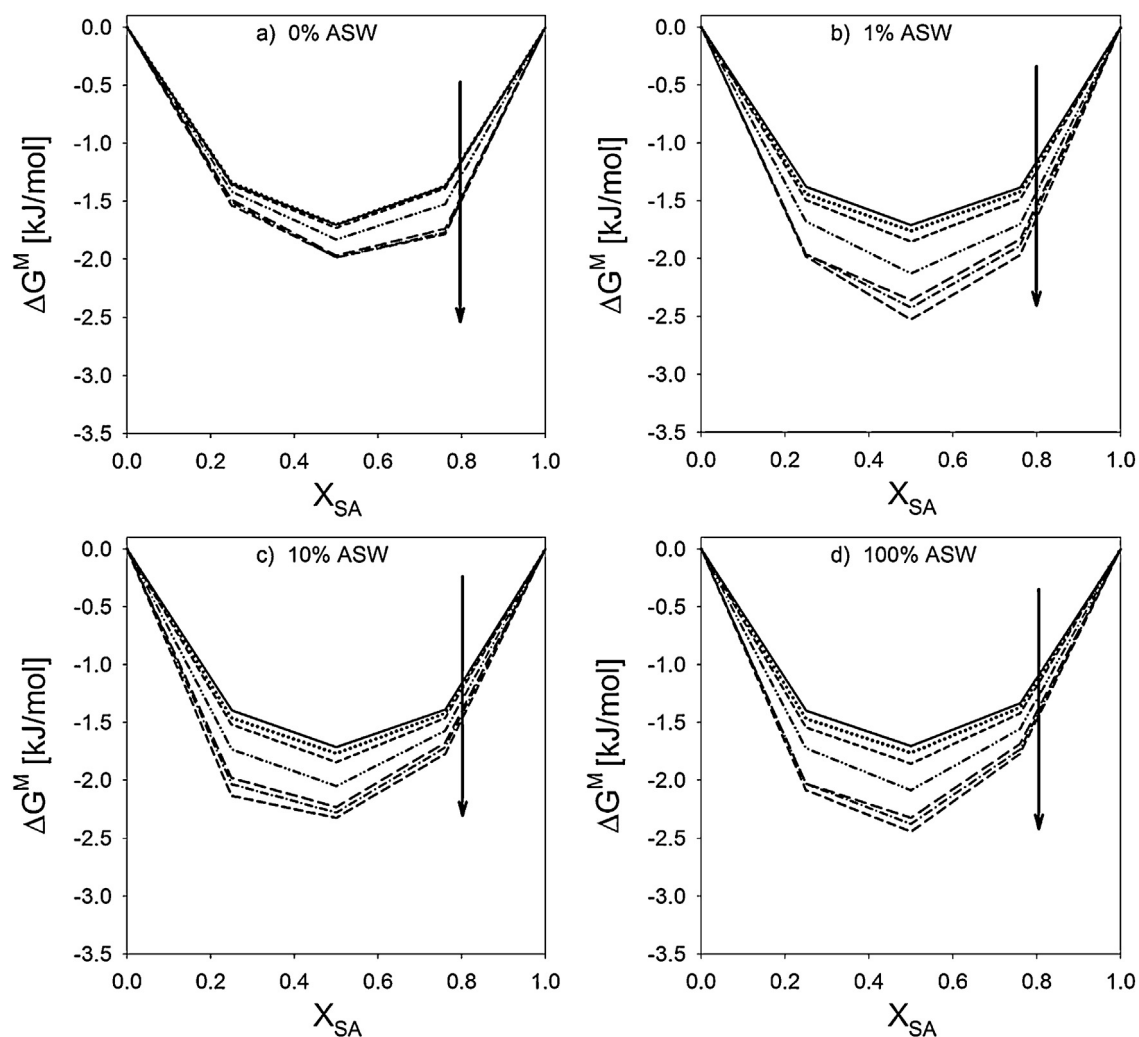


**Fig. 4.** Free energy of mixing ( $\Delta G^M$ ) as a function of molar fraction of stearic acid ( $X_{SA}$ ) in mixed SA:SAm films on various aqueous sub-phases at pH 7. The arrows indicate an increase of the surface pressure. (—) 1 mN/m, (●●●●) 5 mN/m, (---) 10 mN/m, (-●-●-●-) 20 mN/m, (- - -) 30 mN/m, (-●-●-) 40 mN/m, (- - -) 50 mN/m.

and 7 (bottom) for varying  $c_{ASW}$ . At pH 3 the isotherms of the mixed films show a complex signature which does not strongly depend on the salt concentration. This insensitivity to  $c_{ASW}$  corresponds well to a picture in which both SA and PDA are strongly biased towards their protonated state. Since the sub-phase pH is much lower than the (apparent)  $pK_a$  of either species, neither PDA nor SA has a tendency to dissociate and subsequently bind to metal cations from the ASW salt.

The quantitative details of the SA-PDA isotherms (Fig. 7a, c and e) are more difficult to interpret. The first measurable  $\pi$  are found at  $A$ -values in between those of PDA ( $\sim 0.8 \text{ nm}^2$ ) and SA ( $\sim 0.25 \text{ nm}^2$ ). This might suggest weak interactions between PDA and SA. Upon further compression a local maximum  $\pi \sim 24 \text{ mN/m}$ , shortly followed by a minimum at  $\sim 20 \text{ mN/m}$  are observed. The local maximum, interpreted as a fracture pressure, is found between those of pure SA ( $\sim 50 \text{ mN/m}$ ) and PDA ( $\sim 8 \text{ mN/m}$ ). Remarkably, the corresponding value of  $A(\pi_f)$  is much closer to that of pure SA. Considering that the SA fraction alone would give a peak at  $A \sim 0.1 \text{ nm}^2$ , it is clear that significant amounts of PDA are still present at the fracture point ( $\pi_f, A_f$ ), and that this PDA ‘softens’ the average repulsions (as compared to pure SA). Upon further compression, we see a gradual increase in  $\pi$ , ending a quasi-asymptotic rise at  $A \sim 0.05 \text{ nm}^2$ . The latter behaviour resembles that of a pure SA film in the highly condensed state [29], suggesting that in the last stages of compression, (almost) all PDA was depleted from the film.

To further examine the interactions between PDA and SA at pH 3, we calculated the excess mixing areas and energies of the SA:PDA films (see Section 3.1.2). Considering 0%, 1% and 100% ASW sub-phases and  $\pi$  values between 1 and 5 mN/m,  $A_{ex}$  was found to vary between 0 and  $0.065 \text{ nm}^2$  (note the contrast with the SA:SAm mixtures where strongly negative values were found). The excess free energy of mixing (for  $x_{SA} = 0.5$ ) was found to equal  $-1.73 \pm 0.01 \text{ kJ/mole}$ , independent of  $c_{ASW}$  and  $\pi$ . This  $\Delta G^M$  is very similar the ideal value ( $\Delta G^{id} = -1.70 \text{ kJ/mole}$ ), which corroborates our earlier conjecture that SA and PDA show only weak interactions in the mixed films.

We now turn to the behaviour at pH 7. At this pH, the isotherms of the SA:PDA mixed films have essentially similar shapes as those of the pure SA films. However all prominent features in the SA:PDA isotherm are found at much smaller  $A$ : a multiplication by 1.6–2.0 is needed to make them (almost) overlap with the isotherms of the pure SA.

Closer inspection of the isotherms (Fig. 7b, d and f) reveals the following: (i) at large  $A$ , the mixed films exhibit small but significant surface pressures which are not found for films without PDA. This may be due to the relatively ‘bulky’ phenyl group of PDA. In addition the PDA molecules may also more easily adopt a different (e.g. horizontal) orientation due to their lower amphiphilicity. Both mechanisms would explain the noticeable interaction between PDA groups at low surface density. (ii) in the regime where fracture

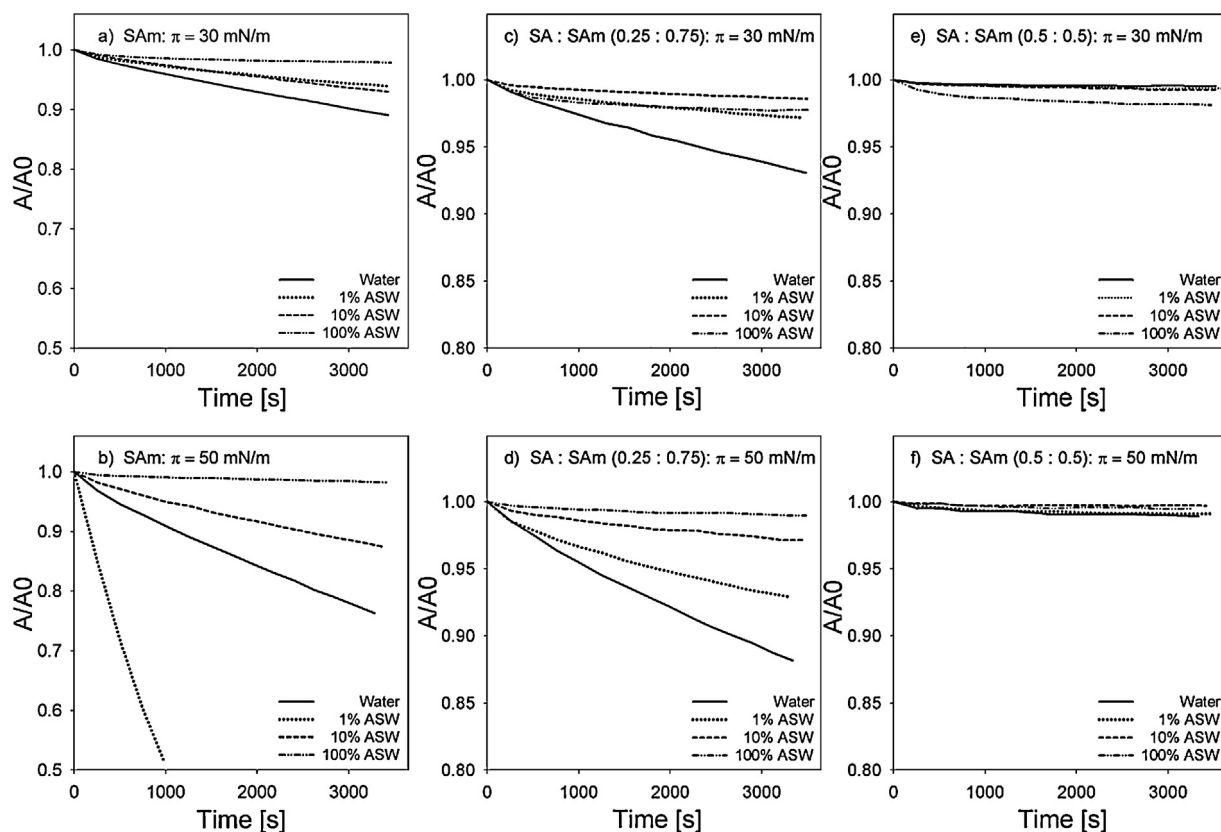


**Fig. 5.** Relaxation curves of SA:SAm films at different mixing ratios, and of pure SAm films determined at  $\pi = 30$  and  $50$  mN/m on sub-phases of pH 7 and varying ASW concentration. Notice different y-axis scale for pure SAm and mixed SA:SAm films.

occurs, the  $\pi_f$  of the mixed film is very close to that of pure SA for  $c_{ASW} = 0\%$  and  $100\%$  (note that at  $1\%$  the  $\pi_f$  of the mixture is even significantly higher than that of pure SA). (iii) for  $c_{ASW} = 100\%$  the pure PDA film is able to sustain surface pressures up to  $\sim 15$  mN/m, indicating a stabilizing effect of sub-phase ASW salt on PDA films. At this  $c_{ASW}$  the SA:PDA mixtures show an increase in the value of  $A$  where  $\pi$  starts to increase steeply; this could be consistent with the stabilizing effect on PDA. We attribute this effect of high  $c_{ASW}$  to a salt-induced deprotonation, leading to the formation of metal–PDA complexes that are more interfacially active than PDA molecules.

The main conclusion from the observations in Fig. 7b, d and f is, however, that at pH 7, the SA and PDA show a rather weak interaction with each other, leading to a strong (almost complete) removal of PDA even during initial compressions of the layer.

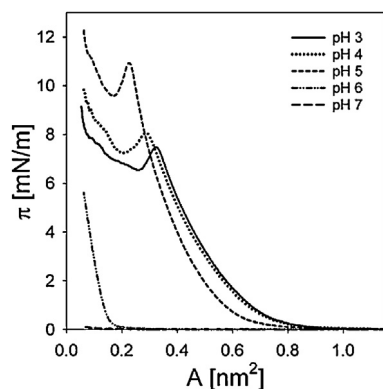


**Fig. 6.**  $\pi$ - $A$  isotherms of PDA. The only electrolytes present in the sub-phase are the HCl or NaOH needed for pH adjustment.

Further characterisation of the weak interaction between SA and PDA via excess mixing areas (as was done for pH 3) was not possible at pH 7 due to the non-quantifiable depletion of PDA from the film.

### 3.2.2. Film relaxation curves of PDA (+SA)

A complementary study of the stability of the PDA and mixed SA:PDA monolayers was conducted by compressing the films to a target pressure and maintaining it via adjustment of the film area (Section 2.2). Pure PDA films could only be analysed at pH 3, due to excessively high loss rates at higher pH. Even at the low pH, the films appeared to be rather unstable. Some trends can be observed in Fig. 8a and b: for the same sub-phase composition, the loss rate increases with  $\pi$  (as expected), and at the same  $\pi$ , the loss rate is lower on a sub-phase of  $100\%$  ASW than on  $0\%$  ASW. However, within the set of curves in Fig. 8a and b, also some non-uniformity is found. At  $\pi = 5$  mN/m,  $A$  decreases at an approximately constant rate, which diminishes as  $c_{ASW}$  is raised from  $0\%$  to  $100\%$ . At  $\pi = 7$  mN/m the relaxation behaviour is more complex. Here, the curve at  $c_{ASW} = 0$  shows a loss rate that grows with time. At  $c_{ASW} = 1\%$  an S-shaped relaxation is observed, while for  $100\%$  ASW the loss rate is more or less constant. The main trend appears to be that ASW-salt stabilises the layer.

Films of PDA mixed with SA were studied also at pH 3 (see Fig. 8c and d). Due to the higher  $\pi_f$  of these mixtures, also higher set point pressures could be maintained. Regarding the effect of increasing  $c_{ASW}$ , we found remarkable differences between the experiments at different surface pressures. At  $\pi = 10$  mN/m, the loss rates were very small and independent of  $c_{ASW}$ : here it appears that the co-presence of SA substantially suppresses the loss of PDA. However at  $\pi = 15$  mN/m it appears that ASW salt has a destabilizing effect on the mixed SA:PDA film. We have no tentative explanation for this.

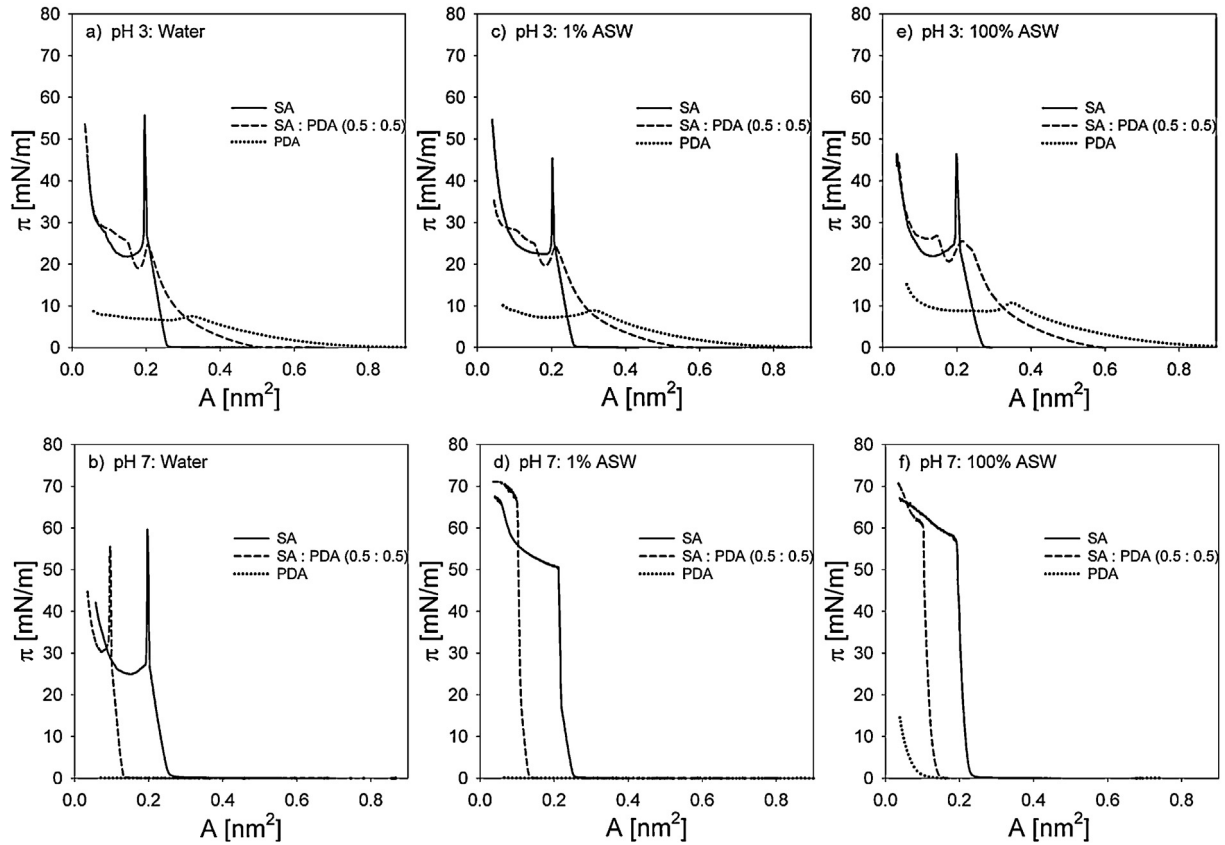


Fig. 7.  $\pi$ - $A$  isotherms of mixed stearic acid (SA) and 12-phenyldodecanoic acid (PDA) films on Artificial Sea Water sub-phase of varying total salt concentration, and pH 3 and 7.  $A$  – area per molecule,  $\pi$  – change of the interfacial pressure upon film compression. The concentration of Na<sup>+</sup> ions in pure water sub-phase due to pH adjustment is 0.09 mM.

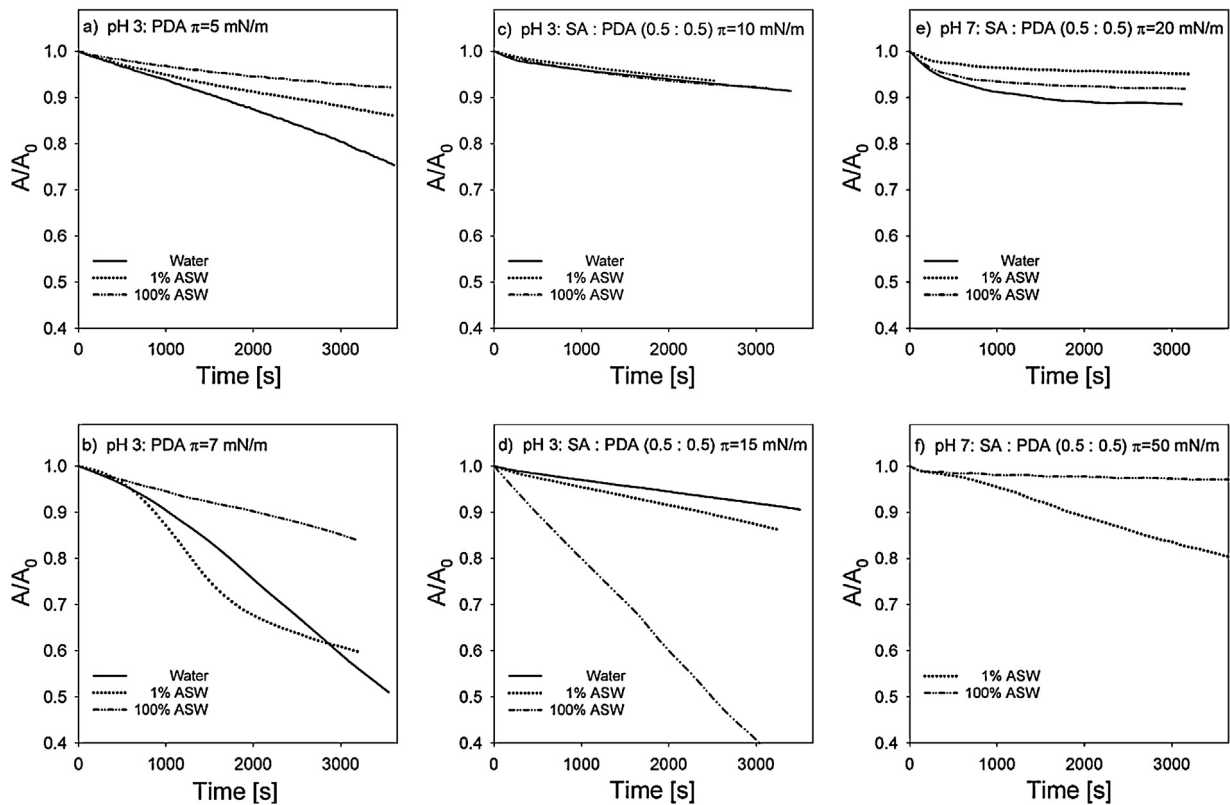


Fig. 8. Relaxation of SA:PDA film on ASW of varying total salt concentration at pH 3.

The observations at  $\pi = 10$  mN/m, where both interfacial SA (compare Fig. 8a and c) and sub-phase ASW (see Fig. 8c) appear to stabilise the interfacial PDA might be explained by a ‘trapping’ effect of the SA, in which the latter (more strongly bound) species surround the PDA molecules, and thereby slow down removal of the latter from the interface. Increasing the  $c_{ASW}$  of the sub-phase could stabilise the interfacial PDA via the formation of metal–PDA complexes as also suggested in Section 3.2.1. Besides that, also the SA molecules get more strongly adsorbed via metal–stearate complexes [29].

Relaxation curves of SA:PDA mixtures at pH 7 strongly resemble these of pure SA films under the same conditions [29]. We observe increase in film stability against molecular loss with increasing  $c_{ASW}$ .

#### 4. Conclusions

We studied the formation and stability of mixed SA:SAm and SA:PDA films on aqueous sub-phases at various (ASW) salt concentrations, and selected pH values. Mixtures of SA with SAm were studied at pH 7, where they can form oppositely charged species. Pressure–area isotherms indicated that SA and SAm are molecularly mixed. Negative excess mixing areas were found, that become larger for increasing salt concentration. However, the corresponding calculated excess free energy of mixing turns out to depend only weakly on the salt concentration. The dependence of this free energy on the SA:SAm mixing ratio turns out to be much stronger, and is most negative when SA and SAm are present in stoichiometric amounts. These trends indicate that the electrostatic attractions between the oppositely charged head-groups are more important than the screening effect of the counter-ions in the sub-phase. Film relaxation experiments corroborated these trends.

The interfacial behaviour of PDA, carrying the same number of carbon atoms as SA, was studied for the first time. The more polar nature of its phenyl group causes PDA to dissolve at pH 7. The presence of SA in the layer and ASW salt in the sub-phase can lower the dissolution rate, but a stable layer is still not obtained. At pH 3 PDA is significantly less soluble, due to the protonation of its head-group. At this pH the interaction with SA turns out to be weak. This is evident from both the isotherms, which indicate an almost ideal mixing, and from the relaxation experiments, which show a slightly increased stability in presence of SA.

#### Acknowledgements

We thank Ian Collins for critical reading of this manuscript and Lei Wang and Naveen Kumar for LB transfers and AFM characterisation. This project was financially supported by BP Ltd.

#### Appendix A. Morphology of mixed SA:SAm films

Additional characterisations of selected mixtures of SA and SAm were performed to reveal the degree of homo- or heterogeneity of the film. To enable high-resolution imaging of the film, Langmuir Blodgett films were prepared on (very flat) oxidised silicon substrates. Transfers were made at  $\pi = 30$  mN/m, i.e. in the steep parts of the isotherms (see Fig. 2). Deposited areas of several cm<sup>2</sup> were inspected with Atomic Force Microscopy (in tapping mode) after drying. This method, elaborately described in ref. [104] allows to identify subtle differences in the local height of the layer and/or its mechanical interaction with the tip. Since the typical lateral range of an AFM scan is restricted to an area of  $O(100 \mu\text{m}^2)$ , several locations on the same sample were examined. The lateral resolution depends on the tip dimensions, but was  $\ll 1 \mu\text{m}$  in our case.

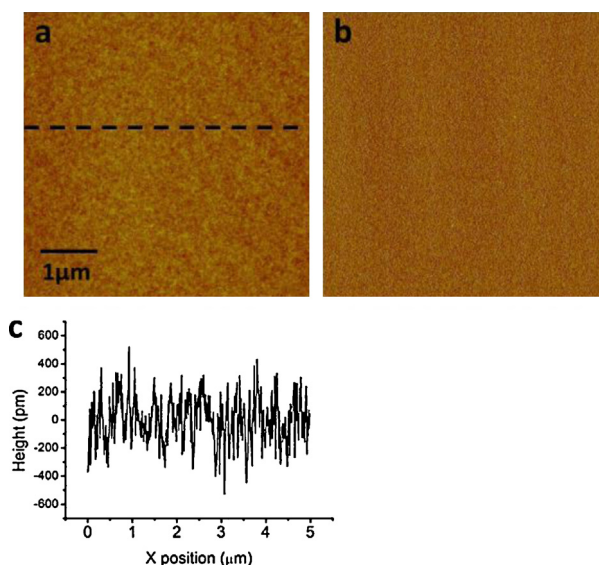


**Fig. A.1.** Morphology of Langmuir–Blodgett film of a 50:50 SA:SAm mixture prepared from a sub-phase of 1% Artificial Sea Water at pH 7. Substrate is an oxidised silicon wafer. Protocols for the LB transfer and AFM imaging are described in [104]. (a) Height image, (b) error image and (c) line profile (dashed line in a). The layer is compact and very smooth with a root mean square roughness of about 0.2 nm.

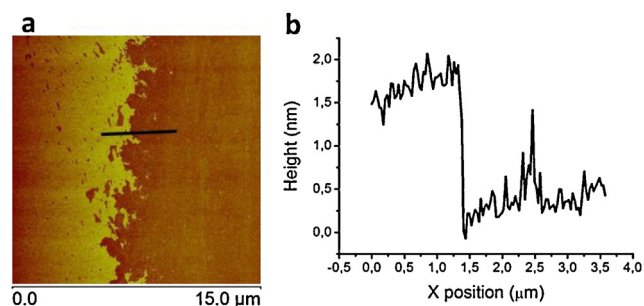


**Fig. A.2.** Height image of the edge of the LB layer (same sample as Fig. 1). The right hand part of the image corresponds to the bare SiO<sub>2</sub> surface. The compact layer has a height of  $1.8 \pm 0.2$  nm, consistent with monolayer coverage. (a) Height image and (b) line profile (solid line in a).

Fig. A.1 shows a representative result for a 50:50 mixture of SA and SAm, obtained from a sub-phase of 1% ASW at pH 7. Both the height map (Fig. A.1a) and error map (Fig. A.1b) look very smooth. As illustrated by the scan line (Fig. A.1c), the noise level is about 0.2 nm. Fig. A.2 shows an image of the edge of the LB layer. It now becomes apparent that the layer has a height of  $1.8 \text{ nm} \pm 0.2 \text{ nm}$ , consistent with the length of stretched SA or SAm chains. Clearly the layer is very dense. Neither differences in height nor domain boundaries were detected. This is consistent with a layer in which SA and SAm are mixed on a molecular level.

#### Appendix B. Supplementary data

Supplementary data associated with this article can be found, in the online version, at <http://dx.doi.org/10.1016/j.colsurfa.2013.04.062>.

#### References

- [1] Morrow, N.R. Wettability, Its effect on oil-recovery, *J. Pet. Technol.* 42 (12) (1990) 1476–1484.
- [2] Y. Liu, J.S. Buckley, Evolution of wetting alteration by adsorption from crude oil, *SPE Formation Eval.* 12 (1) (1997) 5–11.

- [3] S.Y. Lee, et al., Low salinity oil recovery: increasing understanding of the underlying mechanisms, in: SPE Improved Oil Recovery Symposium, Society of Petroleum Engineers, Tulsa, OK, USA, 2010.
- [4] M.A. Ahmadi, S.R. Shadizadeh, Adsorption of novel nonionic surfactant and particles mixture in carbonates: enhanced oil recovery implication, *Energy Fuels* 26 (8) (2012) 4655–4663.
- [5] J.S. Buckley, D.L. Lord, Wettability and morphology of mica surfaces after exposure to crude oil, *J. Pet. Sci. Eng.* 39 (3–4) (2003) 261–273.
- [6] H. Toulhoat, C. Prayer, G. Rouquet, Characterization by atomic-force microscopy of adsorbed asphaltenes, *Colloids Surf. A Physicochem. Eng. Aspects* 91 (1994) 267–283.
- [7] C. Drummond, J. Israelachvili, Fundamental studies of crude oil-surface water interactions and its relationship to reservoir wettability, *J. Pet. Sci. Eng.* 45 (1–2) (2004) 61–81.
- [8] J.S. Buckley, Asphaltene precipitation and crude oil wetting, *Soc. Pet. Eng.* 3 (1995) 53–59.
- [9] I. Kralova, et al., Heavy crude oils/particle stabilized emulsions, *Adv. Colloid Interface Sci.* 169 (2) (2011) 106–127.
- [10] D. Langevin, et al., Crude oil emulsion properties and their application to heavy oil transportation, *Oil Gas Sci. Technol.–Revue De L Institut Francais Du Petrole* 59 (5) (2004) 511–521.
- [11] P.M. Spiecker, et al., Effects of petroleum resins on asphaltene aggregation and water-in-oil emulsion formation, *Colloids Surf. A Physicochem. Eng. Aspects* 220 (1–3) (2003) 9–27.
- [12] G. Alvarez, et al., Small-angle neutron scattering study of crude oil emulsions: structure of the oil-water interfaces, *Langmuir* 25 (7) (2009) 3985–3990.
- [13] G. Alvarez, et al., Heavy oil-water interfacial properties and emulsion stability: influence of dilution, *Energy Fuels* 23 (1) (2009) 294–299.
- [14] S. Poteau, et al., Influence of pH on stability and dynamic properties of asphaltenes and other amphiphilic molecules at the oil-water interface, *Energy Fuels* 19 (4) (2005) 1337–1341.
- [15] T.J. Jones, E.L. Neustadter, K.P. Whittingham, Water-in-crude oil emulsion stability and emulsion destabilization by chemical demulsifiers, *J. Can. Pet. Technol.* 17 (2) (1978) 100–108.
- [16] S. Thomas, Enhanced oil recovery – an overview, *Oil Gas Sci. Technol. – Revue D Iip Energies Nouvelles* 63 (1) (2008) 9–19.
- [17] D.K. Han, et al., Recent development of enhanced oil recovery in China, *J. Pet. Sci. Eng.* 22 (1–3) (1999) 181–188.
- [18] J.S. Huang, R. Varadaraj, Colloid and interface science in the oil industry, *Curr. Opin. Colloid Interface Sci.* 1 (4) (1996) 535–539.
- [19] J.J. Liu, et al., Colloidal interactions between asphaltene surfaces in aqueous solutions, *Langmuir* 22 (4) (2006) 1485–1492.
- [20] Ø. Brandal, et al., Isolation and characterization of naphthenic acids from a metal naphthenate deposit: molecular properties at oil-water and air-water interfaces, *J. Disper. Sci. Technol.* 27 (3) (2006) 295–305.
- [21] H. Aksulu, et al., Evaluation of low-salinity enhanced oil recovery effects in sandstone: effects of the temperature and pH gradient, *Energy Fuels* 26 (6) (2012) 3497–3503.
- [22] R. de Ruiter, et al., Influence of cationic composition and pH on the formation of metal stearates at oil-water interfaces, *Langmuir* 27 (14) (2011) 8738–8747.
- [23] E.L. Nordgard, S. Simon, J. Sjoblom, Interfacial shear rheology of calcium naphthenate at the oil/water interface and the influence of pH: calcium, and in presence of a model monoacid, *J. Disper. Sci. Technol.* 33 (7) (2012) 1083–1092.
- [24] C.Y. Tang, Z.S.A. Huang, H.C. Allen, Binding of Mg(2+) and Ca(2+) to palmitic acid and deprotonation of the COOH headgroup studied by vibrational sum frequency generation spectroscopy, *J. Phys. Chem. B* 114 (51) (2010) 17068–17076.
- [25] S. Kundu, D. Langevin, Fatty acid monolayer dissociation and collapse: effect of pH and cations, *Colloids Surf. A Physicochem. Eng. Aspects* 325 (1–2) (2008) 81–85.
- [26] M. Leonard, R.M. Morelis, P.R. Coulet, Linked influence of pH and cations on fatty-acid monolayer integrity related to high-quality Langmuir-Blodgett-films, *Thin Solid Films* 260 (2) (1995) 227–231.
- [27] S. Xu, K. Miyano, B.M. Abraham, The effect of pH on monolayer stability, *J. Colloid Interface Sci.* 89 (2) (1982) 581–583.
- [28] T.E. Havre, et al., Langmuir films of naphthenic acids at different pH and electrolyte concentrations, *Colloid Polym. Sci.* 280 (7) (2002) 647–652.
- [29] A.M. Brzozowska, M.H.G. Duits, F. Mugele, Stability of stearic acid monolayers on Artificial Sea Water, *Colloids Surf. A Physicochem. Eng. Aspects* 407 (2012) 38–48.
- [30] A. Lager, K.J. Webb, I.R. Collins, LoSal enhanced oil recovery: evidence of enhanced oil recovery at the reservoir scale, in: SPE/DOE Symposium on Improved Oil Recovery, Society of Petroleum Engineers, Tulsa, OK, USA, 2008.
- [31] J.L. Seccombe, G. Jerauld, B. Jhaveri, T. Buikema, S. Bassler, J. Denis, K.J. Webb, A. Cockin, E. Fueg, Demonstration of low-salinity EOR at Interwell Scale, Endicott Field, Alaska, in: SPE Improved Oil Recovery Symposium, Tulsa, OK, 2010.
- [32] T. Hassenkam, et al., The low salinity effect observed on sandstone model surfaces, *Colloids Surf. A Physicochem. Eng. Aspects* 403 (2012) 79–86.
- [33] C.Y. Tang, Z.S. Huang, H.C. Allen, Interfacial water structure and effects of Mg(2+) and Ca(2+) binding to the COOH headgroup of a palmitic acid monolayer studied by sum frequency spectroscopy, *J. Phys. Chem. B* 115 (1) (2011) 34–40.
- [34] M. Maas, et al., On the formation of calcium carbonate thin films under Langmuir monolayers of stearic acid, *Colloid Polym. Sci.* 285 (12) (2007) 1301–1311.
- [35] S. Kundu, A. Datta, S. Hazra, Effect of metal ions on monolayer collapses, *Langmuir* 21 (2005) 5894–5900.
- [36] Ø. Brandal, J. Sjoblom, Interfacial behavior of naphthenic acids and multivalent cations in systems with oil and water. II: formation and stability of metal naphthenate films at oil-water interfaces, *J. Disper. Sci. Technol.* 26 (1) (2005) 53–58.
- [37] O. Brandal, J. Sjoblom, G. Oye, Interfacial behavior of naphthenic acids and multivalent cations in systems with oil and water. I. A pendant drop study of interactions between n-dodecyl benzoic acid and divalent cations, *J. Disper. Sci. Technol.* 25 (3) (2004) 367–374.
- [38] P.A. Kralchevsky, et al., Thermodynamics of ionic surfactant adsorption with account for the counterion binding: effect of salts of various valency, *Langmuir* 15 (7) (1999) 2351–2365.
- [39] R.S. Ghaskadvi, S. Carr, M. Dennin, Effect of subphase Ca<sup>++</sup> ions on the viscoelastic properties of Langmuir monolayers, *J. Chem. Phys.* 111 (8) (1999) 3675–3678.
- [40] J. SimonKutscher, A. Gericke, H. Huhnerfuss, Effect of bivalent Ba: Cu, Ni, and Zn cations on the structure of octadecanoic acid monolayers at the air-water interface as determined by external infrared reflection-absorption spectroscopy, *Langmuir* 12 (4) (1996) 1027–1034.
- [41] P. Koelsch, et al., Specific ion effects in physicochemical and biological systems: simulations, theory and experiments, *Colloids Surf. A Physicochem. Eng. Aspects* 303 (1–2) (2007) 110–136.
- [42] R. Johann, D. Vollhardt, H. Mohwald, Shifting of fatty acid monolayer phases due to ionization of the headgroups, *Langmuir* 17 (15) (2001) 4569–4580.
- [43] A. Datta, et al., Effect of headgroup dissociation on the structure of Langmuir monolayers, *Langmuir* 16 (3) (2000) 1239–1242.
- [44] E. Le Calvez, et al., Effect of cations on the dissociation of arachidic acid monolayers on water studied by polarization-modulated infrared reflection-absorption spectroscopy, *Langmuir* 17 (3) (2001) 670–674.
- [45] B.P. Binks, Insoluble monolayers of weakly ionizing low molar mass materials and their deposition to form Langmuir-Blodgett multilayers, *Adv. Colloid Interface Sci.* 34 (1991) 343–432.
- [46] J.R. Kanicky, D.O. Shah, Effect of degree, type, and position of unsaturation on the pK<sub>a</sub> of long-chain fatty acids, *J. Colloid Interface Sci.* 256 (2002) 201–207.
- [47] R. Aveyard, et al., Stability of insoluble monolayers and ionization of Langmuir-Blodgett multilayers of octadecanoic acid, *Thin Solid Films* 188 (2) (1990) 361–373.
- [48] O. Gershevit, C.N. Sukenik, In situ FTIR-ATR analysis and titration of carboxylic acid-terminated SAMs, *J. Am. Chem. Soc.* 126 (2) (2004) 482–483.
- [49] C. Labbez, et al., Ion-ion correlation and charge reversal at titrating solid interfaces, *Langmuir* 25 (13) (2009) 7209–7213.
- [50] P.M. Dove, C.M. Craven, Surface charge density on silica in alkali and alkaline earth chloride electrolyte solutions, *Geochim. Cosmochim. Acta* 69 (21) (2005) 4963–4970.
- [51] S.H. Behrens, D.G. Grier, The charge of glass and silica surfaces, *J. Chem. Phys.* 115 (14) (2001) 6716–6721.
- [52] M. Wang, A. Revil, Electrochemical charge of silica surfaces at high ionic strength in narrow channels, *J. Colloid Interface Sci.* 343 (1) (2010) 381–386.
- [53] R. Kjellander, et al., A theoretical and experimental-study of forces between charged mica surfaces in aqueous CaCl<sub>2</sub> solutions, *J. Chem. Phys.* 92 (7) (1990) 4399–4407.
- [54] M.D. Heath, B. Henderson, S. Perkin, Ion-specific effects on the interaction between fibronectin and negatively charged mica surfaces, *Langmuir* 26 (8) (2010) 5304–5308.
- [55] J.M. Bloch, W.B. Yun, Condensation of monovalent and divalent metal-ions on a langmuir monolayer, *Phys. Rev. A* 41 (2) (1990) 844–862.
- [56] M. Yazdaniyan, H. Yu, G. Zografi, Ionic interactions of fatty acid monolayers at the air/water interface, *Langmuir* 6 (6) (1990) 1093–1098.
- [57] S. Seok, et al., Imaging of collapsed fatty acid films at air-water interfaces, *Langmuir* 25 (16) (2009) 9262–9269.
- [58] R. Johann, D. Vollhardt, Texture features of long-chain fatty acid monolayers at high pH of the aqueous subphase, *Mater. Sci. Eng.: C* 8–9 (1999) 35–42.
- [59] I. Langmuir, V.J. Schaefer, The effect of dissolved salts on insoluble monolayers, *J. Am. Chem. Soc.* 59 (11) (1937) 2400–2414.
- [60] I. Langmuir, V.J. Schaefer, Composition of fatty acid films on water containing calcium or barium salts, *J. Am. Chem. Soc.* 58 (2) (1936) 284–287.
- [61] S. Kundu, S. Datta, S. Hazra, Effect of metal ions on monolayer collapses, *Langmuir* 21 (13) (2005) 5894–5900.
- [62] M. Yazdaniyan, et al., Divalent-cation stearic acid monolayer interactions at the air-water interface, *Langmuir* 8 (2) (1992) 630–636.
- [63] R.D. Neuman, Stearic acid and calcium stearate monolayer collapse, *J. Colloid Interface Sci.* 56 (3) (1976) 505–510.
- [64] G.S. Patil, D.G. Cornwell, R.H. Matthews, Effect of ionization and cation selectivity on expansion of stearic acid monolayers, *J. Lipid Res.* 13 (5) (1972) 574.
- [65] T. Takenaka, et al., Studies on built-up films by means of the polarized infrared ATR spectrum I.: built-up films of stearic acid, *J. Colloid Interface Sci.* 35 (3) (1971) 395–402.
- [66] A. Matsubar, R. Matuura, H. Kimizuka, A study of interaction between stearic acid monolayer and calcium ions by radiotracer method, *Bull. Chem. Soc. Jpn.* 38 (3) (1965) 369.
- [67] E. Le Calvez, et al., Effect of cations on the dissociation of arachidic acid monolayers on water studied by polarization-modulated infrared reflection-absorption spectroscopy, *Langmuir* 17 (3) (2001) 670–674.

- [68] R. Johann, et al., The effect of headgroup interactions on structure and morphology of arachidic acid monolayers, *J. Phys. Chem. B* 105 (15) (2001) 2957–2965.
- [69] D. June, E.I. Franses, Interactions of charged Langmuir monolayers with dissolved ions, *J. Chem. Phys.* 95 (11) (1991) 8486–8493.
- [70] E. Pezron, et al., Stability of arachidic acid monolayers on aqueous salt solutions, *J. Colloid Interface Sci.* 138 (1) (1990) 245–254.
- [71] V. Dupres, et al., Superlattice formation in fatty acid monolayers on a divalent ion subphase: role of chain length, temperature, and subphase concentration, *Langmuir* 19 (2003) 10808–10815.
- [72] T. Smith, Monolayers on water. 3. Kinetics and mechanism of reaction of erucic acid with copper ions, *J. Colloid Interface Sci.* 25 (4) (1967) 443.
- [73] J.G. Petrov, I. Kuleff, D. Platikanov, Neutron activation analysis of metal ions in Langmuir–Blodgett multilayers of arachidic acid, *J. Colloid Interface Sci.* 88 (1) (1982) 29–35.
- [74] J. Goerke, H.H. Harper, M. Borowitz, in: M. Blank (Ed.), *Surface Chemistry of Biological Systems*, Plenum, New York, 1970, p. 23.
- [75] J.M. Berg, P.M. Claesson, Forces between carboxylic acid layers in divalent salt solutions, *Thin Solid Films* 178 (1989) 261–270.
- [76] O. Albrecht, H. Matsuda, K. Eguchi, Main and tilt transition in octadecylamine monolayers, *Colloids Surf. A Physicochem. Eng. Aspects* 284–285 (2006) 166–174.
- [77] D.W. Westlake, et al., Biodegradability and crude-oil composition, *Can. J. Microbiol.* 20 (7) (1974) 915–928.
- [78] Y.-L. Lee, Y.-C. Yang, Y.-J. Shen, Monolayer characteristics of mixed octadecylamine and stearic acid at the air/water interface, *J. Phys. Chem. B* 109 (10) (2005) 4662–4667.
- [79] N. Schelero, et al., Chain length effects on complex formation in solutions of sodium alkanooates and tetradecyl trimethyl ammonium bromide, *Colloids Surf. A Physicochem. Eng. Aspects* 413 (2012) 115–118.
- [80] R. Zhang, P. Somasundaran, Advances in adsorption of surfactants and their mixtures at solid/solution interfaces, *Adv. Colloid Interface Sci.* 123 (2006) 213–229.
- [81] M.J. Rosen, et al., Ultralow interfacial tension for enhanced oil recovery at very low surfactant concentrations, *Langmuir* 21 (9) (2005) 3749–3756.
- [82] J. Daillant, et al., Elasticity of two-dimensional crystalline monolayers of fatty acid salts at an air–water surface, *Soft Matter* 5 (1) (2009) 203–207.
- [83] K.V. Shaitan, P. Pustoshilov, Molecular dynamics of stearic acid monolayer, *Mol. Biophys.* 44 (3) (1999) 429–434.
- [84] D.J.M. Linden, J.P.K. Peltonen, J.B. Rosenholm, Adsorption of some multivalent transition-metal ions to a stearic-acid monolayer, *Langmuir* 10 (5) (1994) 1592–1595.
- [85] W. Rabinovitch, R.F. Robertson, S.G. Mason, Relaxation of surface pressure and collapse of unimolecular films of stearic acid, *Can. J. Chem.* 38 (1960) 1881–1890.
- [86] G.S. Patil, R.H. Matthews, D.G. Cornwell, Estimation of surface area and counterion binding characteristics in fatty amine monolayers from desorption kinetics, *J. Lipid Res.* 17 (3) (1976) 197–202.
- [87] N.K. Adam, The structure of surface films. Part XV. Amines, *Proc. R. Soc. Lond. A* 126 (802) (1930) 526–541.
- [88] D. Andelman, F. Brochard, J.F. Joanny, Phase-transitions in Langmuir monolayers of polar-molecules, *J. Chem. Phys.* 86 (6) (1987) 3673–3681.
- [89] J.J. Betts, B.A. Pethica, The ionization characteristics of monolayers of weak acids and bases, *Trans. Faraday Soc.* 52 (12) (1956) 1581–1589.
- [90] K.J. Stine, D.T. Stratmann, Fluorescence microscopy study of Langmuir monolayers of stearylamine, *Langmuir* 8 (10) (1992) 2509–2514.
- [91] Y.L. Lee, K.L. Liu, Relaxation behaviors of monolayers of octadecylamine and stearic acid at the air/water interface, *Langmuir* 20 (8) (2004) 3180–3187.
- [92] E.L. Nordgard, et al., Model compounds for C-80 isoprenoid tetraacids Part II. Interfacial reactions, physicochemical properties and comparison with indigenous tetraacids, *Colloids Surf. A Physicochem. Eng. Aspects* 340 (1–3) (2009) 99–108.
- [93] E.L. Nordgard, J. Sjoblom, Model compounds for asphaltenes and C(80) isoprenoid tetraacids. Part I: synthesis and interfacial activities, *J. Disper. Sci. Technol.* 29 (8) (2008) 1114–1122.
- [94] E.L. Nordgard, G. Sorland, J. Sjoblom, Behavior of asphaltene model compounds at W/O interfaces, *Langmuir* 26 (4) (2010) 2352–2360.
- [95] E.L. Nordgard, E. Landsem, J. Sjoblom, Langmuir films of asphaltene model compounds and their fluorescent properties, *Langmuir* 24 (16) (2008) 8742–8751.
- [96] Y. Yoshioka, Photopolymerization in Langmuir–Blodgett films of monoacids containing phenyl and diacetylene groups simultaneously, *Thin Solid Films* 133 (1985) 11–19.
- [97] D.R. Kester, et al., Preparation of Artificial Sea Water, *Limnol. Oceanogr.* 12 (1) (1967) 176–179.
- [98] D.K. Schwartz, Langmuir–Blodgett film structure, *Surf. Sci. Rep.* 27 (7–8) (1997) 245–334.
- [99] M.D. Barratt, Quantitative structure-activity relationships (QSARs) for skin corrosivity of organic acids, bases and phenols: principal components and neural network analysis of extended datasets, *Toxicol. In Vitro* 10 (1) (1996) 85–94.
- [100] P. Ganguly, et al., Role of tail–tail interactions versus head-group-subphase interactions in pressure-area isotherms of fatty amines at the air–water interface. 2. Time dependence, *Langmuir* 13 (20) (1997) 5440–5446.
- [101] F.C. Goodrich, Molecular interaction in mixed monolayers, *Proc. 2nd Int. Cong. Surf. Act.* 1 (1957) 85.
- [102] I.S. Costin, G.T. Barnes, Two-component monolayers, *J. Colloid Interface Sci.* 51 (1) (1975) 106–121.
- [103] L. Ter Minassian-Saraga, Recent work on spread monolayers, adsorption and desorption, *J. Colloid Sci.* 11 (1956) 398–418.
- [104] N.W. Kumar, L. Siretanu, I. Duits, M.H.G. Mugele, Frieder, Salt dependent stability of stearic acid Langmuir–Blodgett films exposed to aqueous electrolytes, *Langmuir* (2013), <http://dx.doi.org/10.1021/la400615j>.